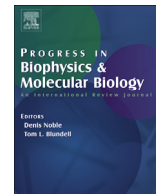




Contents lists available at ScienceDirect

# Progress in Biophysics and Molecular Biology

journal homepage: [www.elsevier.com/locate/pbiomolbio](http://www.elsevier.com/locate/pbiomolbio)

## Removing striping artifacts in light-sheet fluorescence microscopy: a review



Pietro Ricci <sup>a, b, 1</sup>, Vladislav Gavryusev <sup>a, b, 1</sup>, Caroline Müllenbroich <sup>c</sup>, Lapo Turrini <sup>a, b</sup>,  
Giuseppe de Vito <sup>a, d</sup>, Ludovico Silvestri <sup>a, b, e</sup>, Giuseppe Sancataldo <sup>f, \*</sup>,  
Francesco Saverio Pavone <sup>a, b, e, \*\*</sup>

<sup>a</sup> European Laboratory for Non-Linear Spectroscopy, Sesto Fiorentino, 50019, Italy

<sup>b</sup> University of Florence, Department of Physics and Astronomy, Sesto Fiorentino, 50019, Italy

<sup>c</sup> School of Physics and Astronomy, University of Glasgow, G12 8QQ, Glasgow, UK

<sup>d</sup> University of Florence, Department of Neuroscience, Psychology, Drug Research and Child Health, Florence, 50139, Italy

<sup>e</sup> National Institute of Optics, National Research Council, Sesto Fiorentino, 50019, Italy

<sup>f</sup> University of Palermo, Department of Physics and Chemistry, Palermo, 90128, Italy

### ARTICLE INFO

#### Article history:

Received 19 March 2021

Received in revised form

21 June 2021

Accepted 12 July 2021

Available online 15 July 2021

#### Keywords:

Light-sheet microscopy

Striping

3D microscopy

Brain imaging

### ABSTRACT

In recent years, light-sheet fluorescence microscopy (LSFM) has found a broad application for imaging of diverse biological samples, ranging from sub-cellular structures to whole animals, both in-vivo and ex-vivo, owing to its many advantages relative to point-scanning methods. By providing the selective illumination of sample single planes, LSFM achieves an intrinsic optical sectioning and direct 2D image acquisition, with low out-of-focus fluorescence background, sample photo-damage and photo-bleaching. On the other hand, such an illumination scheme is prone to light absorption or scattering effects, which lead to uneven illumination and striping artifacts in the images, oriented along the light sheet propagation direction. Several methods have been developed to address this issue, ranging from fully optical solutions to entirely digital post-processing approaches. In this work, we present them, outlining their advantages, performance and limitations.

© 2021 The Authors. Published by Elsevier Ltd. This is an open access article under the CC BY-NC-ND license (<http://creativecommons.org/licenses/by-nc-nd/4.0/>).

## 1. Introduction

Imaging of biological samples at different scales, ranging from subcellular architecture to whole organisms, has a central role in many fields of biology, since it allows direct observation of fundamental biological structures and processes (Scherf and Huisken, 2015; Wan et al., 2019). Optical microscopes able to capture fast dynamics of biological events in a non-invasive fashion, combined with fluorescent markers for in-vivo selective imaging and with dedicated image analysis programs, are essential tools for quantitative investigation of such biological processes (Power and Huisken, 2017). Novel developments in imaging methods are

crucial to observe and deeper analyse the fundamental interactions happening in biological systems. Within this framework, light-sheet fluorescence microscopy (LSFM) has significantly advanced three-dimensional imaging owing to its relative simplicity and outstanding performance in terms of spatial and temporal resolution (Daetwyler and Huisken, 2016; Engelbrecht and Stelzer, 2006; Fahrbach et al., 2013c). Due to the selective illumination of sample single planes, LSFM provides inherent optical sectioning and direct 2D image acquisition, with small out-of-focus fluorescence background (Huisken et al., 2004; Keller et al., 2008), sample photo-damage and photo-bleaching (Jemielita et al., 2013), whilst guaranteeing high frame rates (Costa et al., 2013; Duocastella et al., 2017; Mickoleit et al., 2014). However, conventional light sheet-based techniques suffer from absorption and scattering by objects within the sample, which results in stripes and shadows along the illumination direction that are apparent in many images presented in the LSFM literature. To mitigate or remove these artifacts which severely affect the image quality, different approaches have been developed, including fully optical solutions and computational

\* Corresponding author.

\*\* Corresponding author. European Laboratory for Non-Linear Spectroscopy, Sesto Fiorentino, 50019, Italy.

E-mail addresses: [giuseppe.sancataldo@unipa.it](mailto:giuseppe.sancataldo@unipa.it) (G. Sancataldo), [pavone@lens.unifi.it](mailto:pavone@lens.unifi.it) (F.S. Pavone).

<sup>1</sup> These authors contributed equally to this work.

post-processing techniques. In this review, after a short introduction to LSFM and the striping effect, we present and discuss in detail these methods.

### 1.1. Light-sheet fluorescence microscopy

LSFM is a three-dimensional optical imaging technique suitable for the study of biological structures and processes in thick samples. The key idea of generating a focused plane of light by illuminating a rectangular thin slit was introduced at the beginning of the 20<sup>th</sup> century by Zsigmondy to improve the imaging performance of optical microscopes designed for colloid analysis (Siedentopf and Zsigmondy, 1903). Although its use for fluorescence imaging was already reported in 1992 by Voie et al. (1993), light-sheet microscopy became popular only after the seminal paper by Huisken et al., in 2004 (Huisken et al., 2004). The technique, also named Selective Plane Illumination Microscopy (SPIM), triggered a revolution in the field of optical microscopy that has greatly facilitated the imaging of large three-dimensional volumes with high resolution and fast acquisition times.

The core idea of LSFM is the combination of an intrinsic optical sectioning excitation scheme with a wide-field detection system. In LSFM, illumination and detection paths are entirely decoupled from each other. In particular, the two optical paths usually have different numerical apertures and working distances optimized for the sample geometry. The light sheet is commonly generated employing a cylindrical lens (Dodt et al., 2007; Huisken et al., 2004) or by rapidly scanning a collimated beam (see digitally-scanned laser light-sheet fluorescence microscopy - DSLM) (Keller et al., 2008; Truong et al., 2011). As depicted in Fig. 1a, light (usually from a laser source), once spatially shaped, completely illuminates the focal plane of the detection system in a direction perpendicular to the observation axis. The sample is placed in the overlapping area of illumination and detection focus. As a result, only signals from this region are detected and no out-of-focus signal contributes to the image formation, resulting in an intrinsic optical sectioning effect. In standard LSFM, to change the imaging plane, the relative position of the observation volume in the sample is translated, allowing to acquire three-dimensional image stacks. The signal is

then collected by the detection system and recorded by a multi-pixel detection device (CCD or sCMOS camera). As a result of the optical sectioning, fluorescence is excited in a thin slice, consequently achieving a high signal-to-noise ratio and imaging contrast. Confocal detection (CLSM) is possibly introduced to further improve those features in images (Baumgart and Kubitschek, 2012; Gavryusev et al., 2019; Medeiros et al., 2015; Silvestri et al., 2012).

Over the last years, LSFM has been adopted worldwide and developed as a useful method for the imaging of thin and extended samples such as fruit flies, larval fish and small mammals in three dimensions (Dodt et al., 2007; Huisken et al., 2004; Keller et al., 2008; Keller and Ahrens, 2015; Mickoleit et al., 2014; Panier et al., 2013; Tomer et al., 2012). Thick and large specimens are commonly chemically treated before volumetric acquisition with optical clearing methods to reduce refractive index mismatch within the sample (Costantini et al., 2015; Silvestri et al., 2016; Ueda et al., 2020). Several reviews describe the fundamental principle and applications of light-sheet microscopy (Chatterjee et al., 2018; Girkin and Carvalho, 2018; Keller et al., 2014; Keller and Dodt, 2012; Santi, 2011; Tomer et al., 2012; Wan et al., 2019; Weber and Huisken, 2011).

### 1.2. Striping artifacts

When imaging biological samples, image degradation deriving from the interaction between light and matter can severely affect the image quality. As represented in Fig. 1b, one of the most common problems is the presence of striping artifacts deriving from lateral illumination of samples.

These artifacts arise from scattering and/or absorption of light by small structures (e.g. impurities, air bubbles, erythrocytes or pigmentation spots) along the single-side illumination light path (Fig. 1c), occluding the light sheet and leading to uneven exposure and reduced fluorescence. Usually, scattering is more relevant in living specimens, where the refractive index is naturally inhomogeneous. In ex vivo samples, clearing methods can be used to reduce or even remove scattering effects (Silvestri et al., 2016). However, light absorption by natural pigments is not affected by

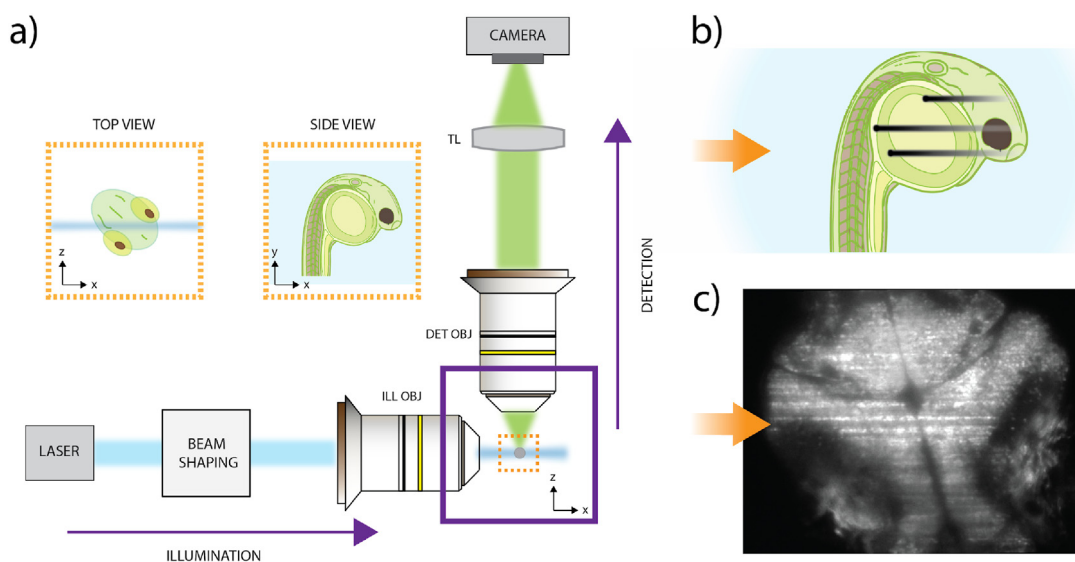


**Fig. 1.** (a) Optical Scheme of LSFM. In light-sheet microscopy, the illumination and the detection are split into two separate light paths. The illumination axis is perpendicular to the detection axis. An objective lens is used to collect fluorescence from the complete field-of-view and maps it on a camera. (b) Cartoon of a typical sample containing optically opaque structural elements illuminated by a single-side illumination approach. Inhomogeneities in the sample (represented by small black dots) lead to artifacts and alterations in LFSM images, resulting in shadows/stripes. (c) Typical one-photon LSFM image of a zebrafish larva where striping artifacts and shadowing are clearly visible. The arrow indicates the direction of light propagation.

most clearing methods (with notable exceptions (Tainaka et al., 2014)). Thus, in general, absorption is the most relevant source of artifacts in cleared specimens, whereas both scattering and absorption contribute in generating shadows in living samples.

Both in live and clarified specimens, the size of scatterers/absorbers is typically quite larger than the wavelength of the illumination laser, since the stripes appear clearly visible in spite of the diffraction limited resolution of the microscope. Consequently, such stripes contribute to poor image quality and lower the signal-to-background ratio (SBR).

Moreover, image analysis, time-correlation investigation, functional mapping and monitoring of biological processes are negatively affected by striping. Reducing the fluorescence variations and spurious features observed during detection allows avoiding incorrect quantitative conclusions or mistakes in biological activity studies.

In the last decade, several effective solutions and useful methods have been proved to address the shadowing effect and usual striping artifacts in LSFM. Here we focused on the analysis of these strategies, presenting first the main optical implementations addressing the problem, then the most promising digital approaches to correct the defects in post-processing and finally widespread hybrid solutions.

## 2. Optical solutions

Optical methods adopted to suppress the striping artifacts in LSFM setups are the first class that we focused on. To get started, we dedicated a first section to self-reconstructing beams, highlighting especially the Bessel beam illumination configuration. Indeed, although simple and straightforward, Gaussian illumination methods usually employed in LSFM show a fundamental limitation: since the illumination beam travels in roughly the same direction confined in a thin sheet, it presents a small angular diversity. Indeed, the maximum light propagation angle is determined by the illumination numerical aperture, which is usually smaller than 0.1 or even 0.01. On the other hand, the incident beam must be tilted enough to surmount the obstacle and avoid shadowing. Improving the range of incidence inclinations guarantees the required angular dispersion to reduce striping, recover information behind the obstructions and increase the image quality.

In a numerical simulation (Rohrbach, 2009), later experimentally validated by following publications from the same group, Rohrbach showed that the strength of striping artifacts depends indeed on the spatial coherence of the incoming sheet of light. Comparing a static light sheet with a digitally scanned one, Rohrbach demonstrates the latter to be less affected by scattering. Thus, we explored multidirectional designs that realize the aforementioned idea by actively moving the illuminating beam. Complementary, the following section covers other pure hardware modifications with respect to conventional SPIM and alternative solutions acting on the spatio-temporal light coherence, adopted to mitigate or partially suppress the striping artifacts. Fig. 2 summarizes the main optical methods most commonly adopted by LSFM setups. The last section collects the advantages and relevant works regarding infra-red excitation in LSFM, intended as an alternative illumination approach applicable to address striping.

### 2.1. Self-reconstructing beams

Among several optical solutions aiming to overcome the drawback of striping formation in LSFM, the use of self-reconstructing beam modes has emerged as an attractive alternative to conventional Gaussian beam illumination. Indeed, self-reconstructing beams, and most notably Bessel beams, have distinct attributes

that make them particularly appealing for microscopy applications. Bessel beams can be generated by an annular aperture placed in the back focal plane of a lens (Durnin et al., 1987; Mcgloin and Dholakia, 2005), by using a conically shaped lens (axicon) (Herman and Wiggins, 1991) or by shaping the phase of an incident Gaussian beam using a spatial light modulator (SLM) (Fahrbach et al., 2010). As depicted in Fig. 2a, the resulting interference pattern shows a lateral intensity distribution comprising concentric rings that are centred around a bright central lobe. Unlike Gaussian beams, Bessel beams propagate over extended distances in a non-diffracting manner (Durnin et al., 1987), maintaining their cross-section invariant over many times the Rayleigh range of a Gaussian beam of equal NA. This propagation invariant feature has led to applications of Bessel beams to extend the depth of field (Ding et al., 2002), the field of view (Fahrbach et al., 2013a) and increase resolution isotropy (Planchon et al., 2011). Fahrbach and colleagues in 2010 first demonstrated the efficacy of using self-reconstructing beams to alleviate striping in a study on light-sheet imaging in scattering and biological samples (Fahrbach et al., 2010). Their work not only gave insights into the physics of complex scattering, but also investigated another important feature of propagation invariant beams, often termed their self-healing ability. When a Bessel beam is blocked or partially obstructed by an object, it can reform itself through interference, thereby recreating the original beam profile behind the obstacle (Garcés-Chávez et al., 2002).

Unlike a Gaussian beam, which carries about 85% of its energy within its  $1/e^2$  waist, the concentric ring system in a Bessel beam contains a large fraction of the total beam energy over a wider transverse area (Fahrbach et al., 2010). Fahrbach et al. showed that, even under conditions of considerable scattering in media with an inhomogeneous refractive index, the photons from the concentric rings converge at the centre of the beam nearly in phase to build a new beam profile. Using a spatial light modulator, the authors directly compare the striping artifacts resulting from diffracted and focused light introduced by Gaussian (DLSM) and SPIM illumination with Bessel DLSM in tissue phantoms and human skin. They demonstrated that Bessel beams produce noticeably better image quality, deeper penetration depths and homogeneous illumination with fewer stripe artifacts than Gaussian beams.

While the Bessel beam ring system is fundamental for the self-healing properties of Bessel beams, the optical energy stored in the rings is also enough to excite fluorescence above and below the focal plane, considerably reducing the SBR in the images. This problem can be alleviated with confocal line-scanning (Fahrbach and Rohrbach, 2012) sectioned Bessel beams (Fahrbach et al., 2013b) or using two-photon Bessel beams (Fahrbach et al., 2013a). Interestingly, confocal line detection using a camera with a rolling shutter, while improving contrast, has been shown to suffer from stronger stripe artifacts for Gaussian beam illumination in scattering media (Meinert et al., 2016). This is due to Gaussian beams being deflected during propagation and no longer propagating parallel to the detection slit after some distance.

Inspired by the aforementioned study of Rohrbach et al. we set out to investigate the detrimental effects of illumination artifacts in two research fields pursued in our laboratory, namely the reconstruction of the neuronal and vascular cyto-architecture in intact clarified mouse brains and calcium imaging of spontaneous neuronal activity in zebrafish larva. Using an axicon and a phase mask in a custom-made light-sheet microscope (Müllenbroich et al., 2015), our lab has demonstrated the suppression of striping artifacts when imaging whole clarified mouse brains. We found that even in extremely well optically cleared samples, residual refractive index heterogeneities lead to severely striated images in 30% of the brain volume.

Furthermore, a significant amount of information content

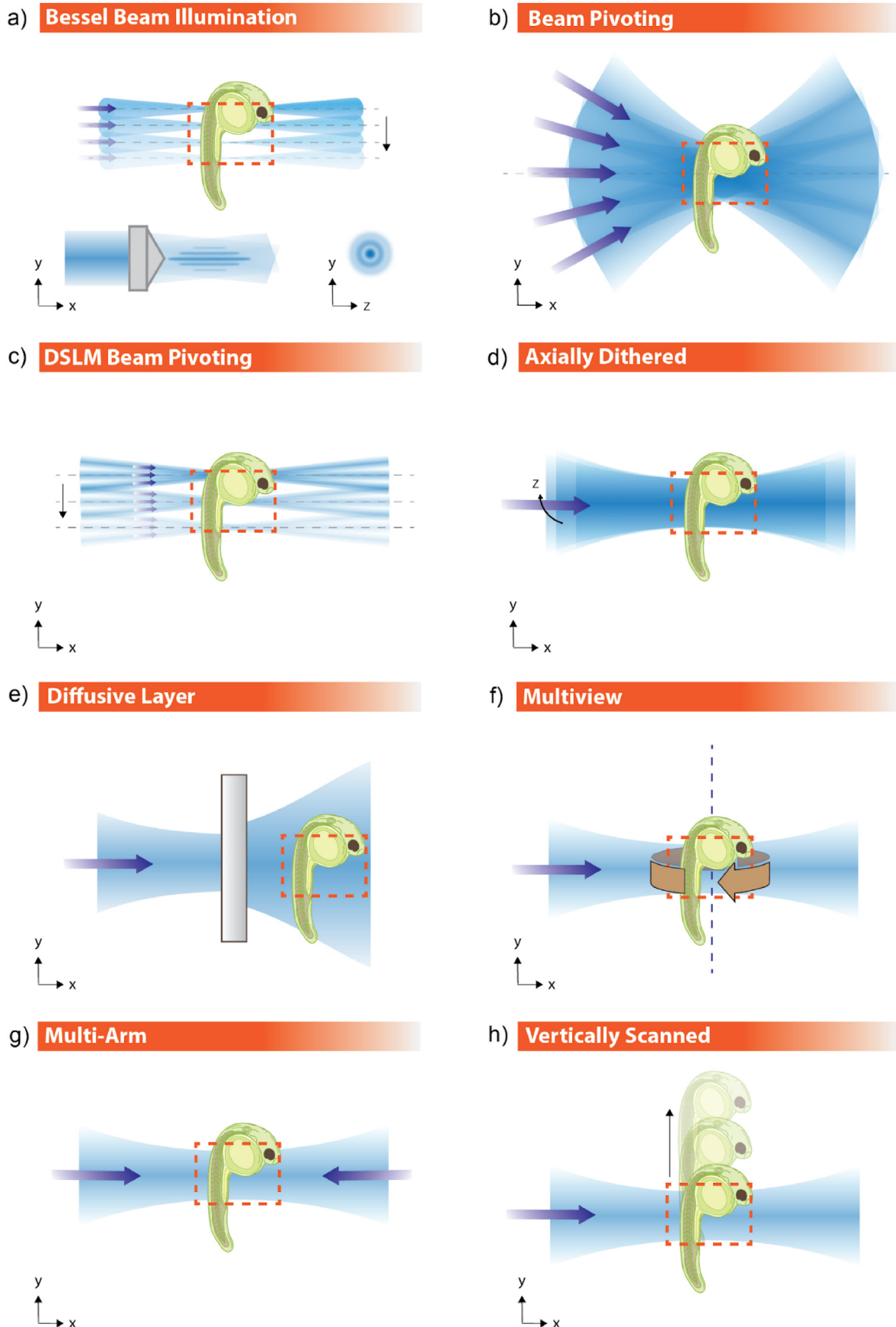


**Fig. 2.** Schematic of optical methods adopted in LSFM to remove striping artifacts. Blue arrows indicate light propagation direction. Orange dotted lines indicate the detection field of view.

irreversibly lost with Gaussian DLSM was accessible when interrogated with Bessel beams. This beam mode produced high-fidelity structural data of improved image homogeneity, allowing for the automated segmentation of blood vessels by simple thresholding in areas otherwise completely obscured by shadows using Gaussian illumination (Müllenbroich et al., 2018a). The use of Bessel beams has thus the potential to significantly relax demands placed on the automated tools to count, trace or segment fluorescent features of interest.

Another example of data analysis affected by striping artifacts has been investigated by comparing Gaussian and Bessel illumination in zebrafish imaging (Fig. 3). In addition to aforementioned static shadows (Fig. 3a–d), during brain functional imaging, hemodynamic artifacts are caused by blood cells passing through the light sheet which causes them to transiently scatter and absorb the excitation light. Their shadows dynamically modulate the fluorescence intensity, causing an artifact we termed “flickering”. Since during  $\text{Ca}^{2+}$  imaging variations of fluorescence signal over time quantify neuronal activity, flickering artifacts caused by moving ghost images cause loss and/or corruption of data obtained in light-

sheet microscopy experiments, forcing for example a previous study to manually exclude from further analyses neurons affected by severe flickering (Panier et al., 2013).

We demonstrated this corruption of correlation in neuronal activity by direct comparison between Bessel and Gaussian DLSM (Fig. 3e–h). We found a fivefold increase in sensitivity to calcium transients and a twenty-fold increase in accuracy in the detection of activity correlation in functional imaging with Bessel beams (Müllenbroich et al., 2018b). Furthermore, we demonstrated that Bessel beams can reveal strong correlations (otherwise lost when using Gaussian illumination) in one-shot measurements, such as the investigation of spontaneous activity, which preclude the possibility to clean up data by averaging of repeated trials.

Recently, Kafian and collaborators (Kafian et al., 2020) demonstrated the efficacy of another non-diffracting beam mode, the Airy beam (Siviloglou et al., 2008; Vettenburg et al., 2014), in increasing the image quality of biological samples. They exploited the self-healing and penetration properties of a 2D Airy beam to perform volumetric imaging of nuclear-stained dense mammospheres of cancer cells.

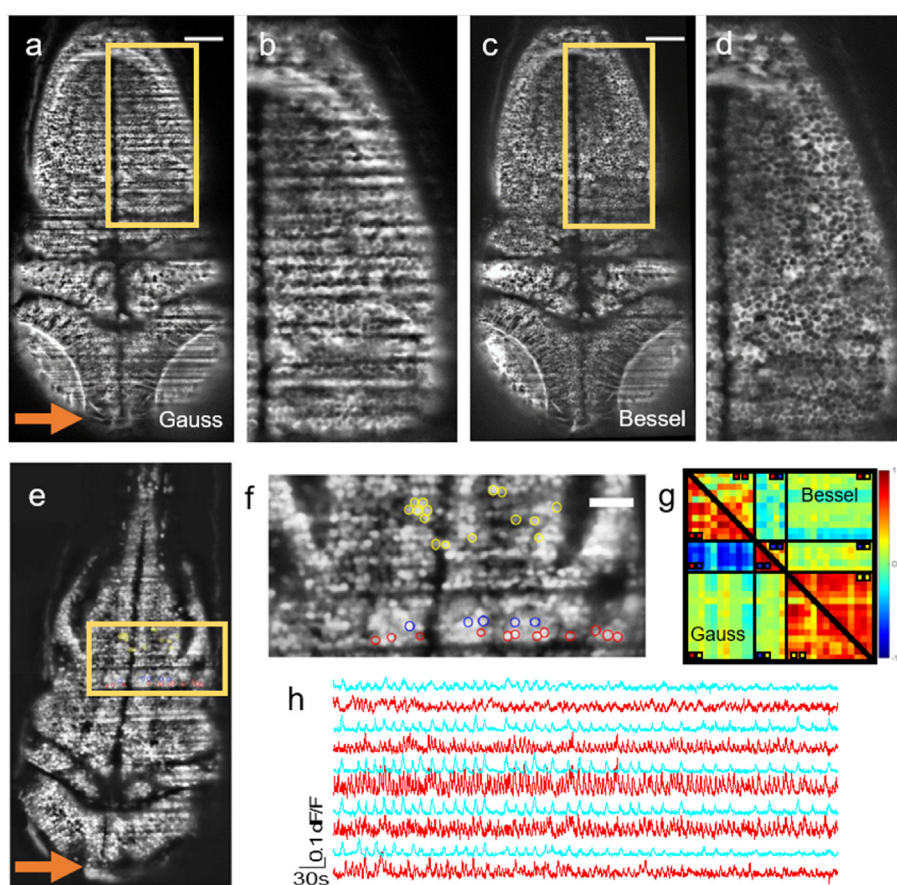


**Fig. 3.** Comparison of Bessel and Gaussian illumination for striping artifact suppression in zebrafish imaging. (a, c) Static shadows in the encephalon of a 3 dpf *Tg(elavl3:GCaMP6s)* zebrafish with cytoplasmic expression of GCaMP imaged with Gaussian (a) and Bessel (c) beam illumination. The orange arrow indicates light sheet propagation. Scale bars: 100  $\mu\text{m}$ . (b, d) Magnifications of the yellow rectangles from (a, c), respectively, showing the hindbrain. The contrast in both images has been enhanced over the entire image using Contrast-Limited Adaptive Histogram Equalization (CLAHE) in ImageJ for better visualization. (e) Horizontal plane of a 4 dpf larva imaged with Gaussian illumination, the yellow rectangle indicates the zoomed-in panel shown in (f). In (f) cells located on two adjacent excitation lines are indicated in red and blue. The striping shadow affects all cells in one line simultaneously. Cells randomly selected in the hindbrain and part of an active network are indicated in yellow. (g) Correlation matrix of cells measured with Gaussian (lower triangular) and Bessel beam illumination (upper triangular matrix). The colour scale ranges from  $-1$  (blue) to  $+1$  (red). In the Gaussian case, note the strong correlation between red cells (area denoted with two red squares) and the strong anticorrelation between red and blue cells (area denoted with a red and a blue square). Both are examples of corrupted correlation. (h) Representative traces of the cells marked in yellow in (f) measured with Gaussian (red) and Bessel (cyan) beam illumination. Traces measured with Bessel beam illumination are subject to less noise and have an increased sensitivity to calcium transients. Figure adapted with changes from (Müllenbroich et al., 2018b); Marie Caroline Müllenbroich, Lapo Turrini, Ludovico Silvestri, Tommaso Alterini, Ali Gheisari, Natascia Tiso, Francesco Vanzi, Leonardo Sacconi, Francesco Saverio Pavone, “Bessel Beam Illumination Reduces Random and Systematic Errors in Quantitative Functional Studies Using Light-Sheet Microscopy,” *Frontiers in cellular neuroscience* 12 (2018): 315, © 2018 Müllenbroich, Turrini, Silvestri, Alterini, Gheisari, Tiso, Vanzi, Sacconi and Pavone. Figure distributed under the terms of the Creative Commons Attribution License (CC BY).

## 2.2. Multidirectional illumination

An early clever solution to the striping problem was the pivoting of the light sheet (multidirectional SPIM or mSPIM) (Huisken and Stainier, 2007), obviating the lack of angular diversity of SPIM in a simple way. In such a configuration, the light sheet, which propagates from the illumination objective, is pivoted in the detection focal plane within a range of angles (Fig. 2b). As reported in (Sancataldo et al., 2019), our group discussed the pivoting dynamics required to achieve efficient shadow suppression within each camera exposure. Even if, with respect to static light-sheet illumination, good results can be obtained with a single scanning cycle within the framerate of the imaging camera, we demonstrated that image artifacts are still evident using slow sweeping rates, while they are greatly reduced at higher rates, averaging out the shadows over time, and resulting in an enhanced uniform illumination.

The idea of multidirectional pivoting has been successfully translated to the DSLM configuration. Indeed, a simple and passive multidirectional digital scanned light-sheet microscopy (mDSLMS) architecture that combines the benefits of mSPIM and DSLM has been developed by Glaser et al. (2018). mDSLMS tackles the need for angular diversity by shaping the excitation beam in an elliptical Gaussian beam with increased angular diversity. Thus, mDSLMS provides mitigation of shadowing artifacts of fluorescently labeled samples while preserving the image contrast enhancement provided by confocal line detection without beam pivoting.

In multidirectional light-sheet microscopy, pivoting is commonly achieved by employing a galvanometric mirror (GM) placed in a conjugate plane that can rotate around the optical axis. This strategy to reduce illumination artifacts, however, could compromise the acquisition speed since the light sheet has to be pivoted within a single image acquisition or within a single line detection. Moreover, the speed of galvanometric mirrors is limited by the inertia to an upper bound in the range of about 200 Hz. Imaging of faster events is usually obtained by means of resonant mirrors, capable of faster scanning dynamics up to 8 KHz, even if limited by a fixed scanning speed.

Furthermore, with modern sCMOS sensors, the line exposure times in rolling shutter modality can be as short as 10  $\mu$ s, corresponding to sweeping rates of 100 kHz. This camera modality results particularly used in CLSFM, as mentioned in the introduction, to increase the image signal-to-noise ratio (SNR) and contrast, rejecting out-of-focus and scattered light. Therefore, to keep up to the state-of-the-art readout rate offset between adjacent row exposures, we accordingly need faster pivoting dynamics, even larger than the ones achievable with resonant mirrors.

For this reason and to overcome constraints imposed by the inertia of mechanical components, our group recently reported the use of Acousto-Optic Deflectors (AODs) in multidirectional SPIM (Sancataldo et al., 2019) and DSLM (Ricci et al., 2020) configurations as schematically represented in Fig. 2c. Fig. 4 shows a comparison between images taken with standard Gaussian illumination with the ones taken while pivoting the beam by an AOD in DSLM, highlighting with orange arrows the areas where striping artifacts were suppressed. AODs avoid the need for any mechanical movement to scan a laser beam, thus removing the inertia constraint and enabling MHz pivoting rates. Interestingly, AODs allow for the simultaneous generation and independent intensity control of a series of multiple beams from a single laser beam. Thus, by means of a single AOD it is possible to create multiple static light sheets coming from tuneable different angles, obtaining even a doubling of the imaging speed (Gavryusev et al., 2019), or to pivot a single light sheet at rates unattainable with a galvanometric mirror.

## 2.3. Alternative optical approaches

An alternative approach to achieve three-dimensional imaging is tilting the beam laterally with proper scanning mirrors enabling light-sheet microscopy without additive optics. In DSLM, for the first time introduced by Keller et al. (2008), the specimen is easily light-sectioned, and an image stack can be obtained faster. A dutiful analysis of the advantages provided by DSLM, compared with previous LSFM versions, has been carried out by Pampaloni et al. (2011) through the imaging of cellular spheroids, addressing the larger penetration depth achievable, the deconvolution performance and especially the stripe artifact reduction in the light-sheet illumination. Once they demonstrated how DSLM is the ideal tool for imaging deep inside large three-dimensional cell cultures, evaluating the resolution and signal-to-noise ratio (SNR) enhancement, they also highlighted the convenience provided in terms of shadow attenuation.

Several alternative optical solutions have been implemented to improve the DSLM performance. On the heels of what has been reported concerning the multidirectional approach, a recent work provided by Liu et al. (2019) has led to the successful development of a method for alleviating such shadowing, compatible with DSLM and structured illumination DSLM-SI. They realized an axially dithered digital scanned light-sheet microscope (aDSLMS) and demonstrated to improve by 20% the striping reduction, in terms of intensity standard deviation, compared to DSLM. This approach can be easily implemented by dithering the illumination beam by a small angle (less than  $0.03^\circ$ ) along the axial direction, i.e. the detection axis (Fig. 2d). The beam is scanned by a dual-axis galvo-mirror, synchronizing one scanning dimension with the rolling shutter of the camera to exploit the confocal detection contrast enhancement.

A geometrically alternative setup is the one implemented by Dean et al. (2016) where the advantages carried by their diagonally swept light-sheet microscope DiaSLM are highlighted in terms of improved sensitivity, decreased sample irradiance, diminished photobleaching and enhanced illumination uniformity with respect to other LSM approaches. In this configuration, the sample is mounted at  $45^\circ$  relative to the excitation and the detection directions. By placing a custom amplitude-grating conjugate to the sample plane in the illumination path, they created a series of superimposed Gaussian beams (i.e. a Gaussian lattice) which cover a much larger solid angle than, for example, a beam generated from a cylindrical lens. The Gaussian lattice is then dithered across the field of view with a galvanometric mirror, to generate a time-averaged light sheet which severely improves the illumination evenness and attenuates the shadow artifacts.

An alternative to beam scanning or dithering to effectively create a time-averaged superposition of incoherent light sheets, is the one recently proposed by Ren et al. (2020). Their novel approach - called coded light-sheet array microscopy (CLAM) - allows complete parallelized 3D imaging without mechanical scanning, minimizing the illumination artifacts originated in highly scattering tissue. In particular, they generated an incoherent superposition of a light sheet array with controllable sheet density and degree of spatial coherence, exploiting the multiple reflections between an angle-misaligned mirror pair.

Another option acting on the light spatial coherence is the one proposed by Calisesi et al. (2019). By exploiting a Digital Micromirror Device (DMD) illuminated by an incoherent LED source, they obtained a spatially modulated light sheet able to artifact-free sample volumetric reconstruction. Despite their claim for further modulation optimization requirements to study fast biological processes, they proved their novelty by imaging living zebrafish

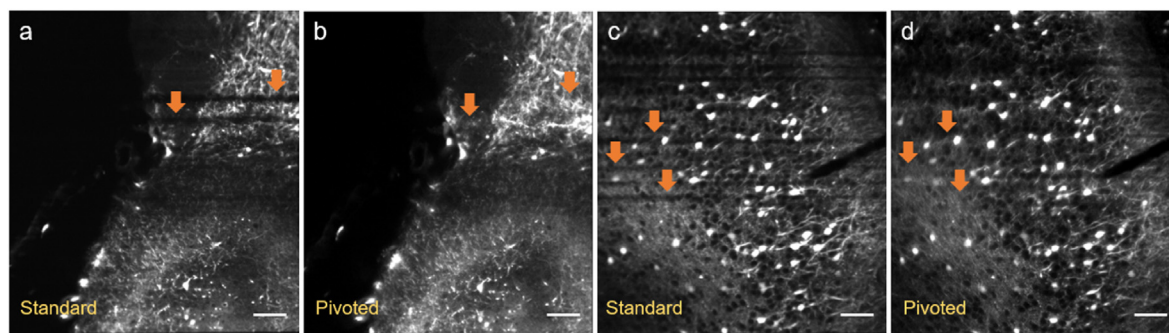


**Fig. 4.** Stripping artifacts suppression. (a,c) Show single frames acquired in two different mouse brains expressing fluorescent protein tdTomato, taken in standard configuration with Gaussian illumination. (b,d) Show the same view taken with AOD pivoted beam configuration. Areas of larger striping attenuation are indicated by orange arrows. Scale bar is 100  $\mu\text{m}$ . Figure adapted with changes and permission from (Ricci et al., 2020): Pietro Ricci, Giuseppe Sancataldo, Vladislav Gavryusev, Alessandra Franceschini, Marie Caroline Müllenbroich, Ludovico Silvestri, Francesco Saverio Pavone, “Fast multi-directional DSLM for confocal detection without striping artifacts” *Biomed. Opt. Express* 11, 3111 (2020). <https://doi.org/10.1364/BOE.390916>. © 2020 Optical Society of America.

embryos avoiding unwanted speckle patterns and shadowing effects.

In this regard, Merino et al. and Di Battista et al. (Di Battista et al., 2019; Merino et al., 2015) also contributed a striping reducing solution by deteriorating the illumination beam spatio-temporal coherence in their elastic scattering light-sheet microscopy. They first lowered the temporal coherence of the light beam by implementing a supercontinuum fibre laser with large emission bandwidth and, to act also on the spatial coherence, they improved the angular diversity by pivoting the light sheet using a GM before the pupil of the illumination objective.

A different optical approach is the one proposed by Taylor et al. (2018): a diffuse digitally scanned light-sheet (dDSLS). The authors introduced a line diffuser in a light-sheet microscope through which the incident light is spread across the full angular range (Fig. 2e). It produces freely crossing incident rays, subsequently focused by the illumination objective. The resulting randomized light allows the light sheet to restore after obstructions instead of creating shadows behind. Even if an analysis in terms of resolution and contrast compared with other well-known approaches is still missing, it has been demonstrated that striping artifacts were severely reduced, both in SPIM and in a DSLM configuration. However, randomizing the coherent laser light generates laser speckles, resulting in a heterogeneous illumination field that degrades image quality. To avoid this shortcoming, the diffuser has to be moved laterally faster than the imaging rate in order to shift around the speckle pattern, inducing a more uniform illumination field due to time averaging. Such an approach is hardly compatible with the confocal detection modality because the diffuse light illumination breaks the requirement of having a single illumination line sweeping synchronously with the filtering digital slit.

A slightly different approach is the one proposed by Salili et al. (2018) who successfully demonstrated prevention of stripes formation by introducing, before the sample, an elliptical holographic diffuser (EHD) over the incident light-sheet. Instead of an ordinary diffuser (commonly circular), the use of an EHD provides anisotropic transmitted light (i.e. depending on the mutual orientation of the light sheet and the elliptical diffuser). Furthermore, the diffuser texturized surface has a pseudo-random morphology pattern which allows the light to diffuse without creating a speckle pattern.

#### 2.4. Infrared illumination LSFM

As originally demonstrated by Lord Rayleigh, the amount of elastic scattering undergone by light when it encounters particles much smaller than its wavelength is inversely proportional to the

fourth power of its wavelength (Young, 1981). Consequently, the Rayleigh-type scattering component (but not the Mie-type nor the geometric one) is significantly reduced by using infrared instead of visible light excitation. Furthermore and even more importantly, the use of a longer illumination wavelength allows working in an optimal biological window (between 650 nm and 1200 nm) where autofluorescence is low and hemoglobin, water, and protein absorption are depressed, greatly improving the penetration of excitation light in the sample, thus granting a more homogeneous illumination. These are the reasons why microscopy techniques based on two-photon (2P) absorption of near infrared light are particularly suited for imaging in thick specimens with respect to their one-photon (1P) variants, as specifically demonstrated for 2P LSFM (Lavagnino et al., 2013, 2016).

The significantly reduced absorption and suppressed Rayleigh-type scattering also imply that imaging by 2P LSFM would be characterized by a low probability of shadowing, making multiphoton excitation a good candidate to face the striping issue. Nevertheless, a rigorous experimental comparison between the two modalities on this topic is still lacking, even though microscopes able to seamlessly switch between these two operating modes were already reported (Lavagnino et al., 2013, 2016; Lemon et al., 2015; Tomer et al., 2012; Truong et al., 2011; Wolf et al., 2015). Anyway, an inspection of the published 2P LSM literature (Cella Zanacchi et al., 2011; Lavagnino et al., 2013, 2016; Lemon et al., 2015; Palero et al., 2010; Tomer et al., 2012; Truong et al., 2011; Wolf et al., 2015) does not show the presence of strong striping artifacts. Similarly, we did not observe such issues either during our 2P LSM acquisitions (de Vito et al., 2020a, 2020c). This suggests an effective stripe mitigation effect induced by the use of infrared illumination light.

Recently, new technical developments in LSFM have been presented pushing the illumination light wavelength further in the infrared region, exploiting either three-photon absorption of 1000-nm light (Escobet-Montalbán et al., 2018) or fluorophores with longer excitation (1320 nm)—and emission (1700 nm)—wavelengths (Wang et al., 2019). This longer-wavelength light is associated with even more reduced scattering. In fact, Wang et al. (2019) report that LFSM with both excitation and emission in the near-infrared II window avoids striping artifacts.

It should be noted that, while the other infrared-illumination-based approaches are still prone to imaging artifacts produced in the detection path, the latter is more robust in this aspect, thanks to the concomitant use of infrared light in emission. On the other hand, a disadvantage of using infrared light with 1P excitation is a

significant reduction of the achievable optical resolution, due to the enlargement of the detection and excitation PSFs. Differently, with multiphoton excitation this effect is greatly reduced, since the nonlinear interaction limits the excitation PSF size and induces the generation of shorter wavelength fluorescence light.

### 3. Digital solutions and post-processing approaches

Digital processing of images is an alternative solution to suppress striping artifacts with respect to optical methods. Instead of increasing the complexity of the optical setup, it relies on the use of algorithms and computational processing to automatically identify and remove within the images the stripe defects, while minimally affecting the useful signal. Digital processing methods can be employed when it is possible to distinguish and separate within the acquired data what constitutes the signal from the noise contributions, using one or more criteria. This approach can be applied either as a post-processing step, without imposing additional requirements on the measurement setup, or even in real-time if sufficient computational power is available to perform the calculations within a single measurement cycle.

The nature of the striping artifacts that affect LSM can be assimilated to spatially correlated, multiplicative noise because they originate from the attenuation or scattering of the excitation light by objects located within the sample. This kind of noise is very different from the uncorrelated, additive noise whose distribution is independent from the sample, like white or instrumental noise that is more frequently addressed by denoising algorithms (Krull et al., 2020; Mandracchia et al., 2020; Peng et al., 2017) or as stripes spanning entire image columns or rows which are handled by uneven illumination compensation methods (Smith et al., 2015; Teranikar et al., 2020; Uddin et al., 2011). As a result, only a few specific solutions for multiplicative noise are currently available, but it is still possible to apply methods developed for additive noise by taking the logarithm of the image data, performing the filtering and converting back to the original scale.

Striping, either as an additive or multiplicative noise contribution, is a problem shared among many other imaging techniques such as satellite imaging, where it has been addressed via histogram moment matching (Gadallah et al., 2000; Rakwatin et al., 2007) and a Bayesian maximum a posteriori method (Shen and Zhang, 2009), focused ion beam nanotomography and synchrotron-based X-ray microtomography, where a combined wavelet-Fourier filtering was demonstrated (Münch et al., 2009). It is also encountered in atomic force microscopy and imaging with passive millimeter-waves or moderate resolution spectroradiometers, where it has been corrected via FFT filtering (Chen and Pellequer, 2011) or an advanced unidirectional total variation and framelet regularization approach (Chang et al., 2013). All these techniques are potentially applicable to LSM. In particular, striping artifacts affect several other optical microscopy modalities, that are closer in nature to LSM, and in these cases, it has been remedied through custom pipelines leveraging moving median filtering (Ding et al., 2013) or Sobel filtering and polynomial fitting (Pollatou, 2020).

Since the stripes share the same angular orientation and an oblong morphology, in principle they could be easily suppressed by using a bidimensional band-pass Fourier filter. It is simple to implement and computationally fast, however, this approach is not very effective. The reason is that, if the applied attenuation is excessive or too wide, it can blur or even conceal important features of the sample that may be encoded along the same orientation angle in the filtered frequency band. While, in the opposite case, stripes may not be completely removed. For this reason, more complex and effective approaches have been developed.

Leischner et al. (2010) demonstrated the efficacy of an approach developed starting from the rolling ball algorithm (Sternberg, 1986), a well-known technique used for processing medical images. This approach is based on the combination of simple mathematical morphology operations, such as the sequence of a one-dimensional closing followed by a one-dimensional opening (Dougherty Edward, 1992), to obtain the local illumination of every pixel. This technique showed to be very effective and it is also able to compensate for local illumination inhomogeneities. However, it requires manual tweaking of parameters such as the size of the neighbourhood used for the mathematical morphology operations.

A theory-based solution was proposed by Uddin and colleagues (Uddin et al., 2011) where they applied radiative transfer theory to model light propagation, absorption and emission within the imaged samples and the subsequent image formation process. They have shown that considering only attenuation allows improving illumination homogeneity, while stripes can be mitigated by including re-emission of the light absorbed by the fluorophores.

Fehrenbach and co-workers have demonstrated that additive stationary stripe noise can be efficiently removed using variational stationary noise removing algorithms (VSNR) that perform a maximum a posteriori filtering within a Bayesian framework (Fehrenbach et al., 2012). Subsequently, this method was extended to address multiplicative noise by Escande and collaborators (Escande et al., 2017). In their work, the striping artifacts are modelled as stochastic stationary processes and a maximum a posteriori estimate is used to recover the destriped image. The heavier computational load is compensated by an optimized and parallelized implementation for graphical processing units.

A significant refinement of the Fourier filtering approach, named multidirectional stripe remover (MDSR), has been developed by Liang and collaborators (Liang et al., 2016). They have combined a non-sampled contourlet transform, that is shift-invariant and decomposes the image into several directional subbands, with multidirectional Fourier-filtering, achieving good selectivity and avoiding blurring while performing as well as VSNR. An example of destriping results obtained by applying the MDSR (Liang et al., 2016), VSNR (Fehrenbach et al., 2012) and wavelet-FFT (Münch et al., 2009) algorithms on an LSM image of colon affected by striping is presented in Fig. 5. All three methods can remove most of the stripes, even if for the specific input image wavelet-FFT suffers from blurring and VSNR displays few residual artifacts, contrary to MDSR.

Digital image processing has been used not only as a standalone tool or within analysis pipelines, but it has been also combined with optical methods, both for noise suppression purposes and for mitigation of illumination inhomogeneity and sample attenuation, as discussed in the following section.

### 4. Hybrid solutions

In this section we focus the attention on several hybrid approaches that involve hardware optical advancements with respect to the classical SPIM technique, but also that exploit post-processing methods or volumetric data stitching to improve the image quality.

An effective solution to the striping issue is represented by the multiple view imaging of the sample (Swoger et al., 2007). As depicted in Fig. 2f, multiview is achieved by volumetrically imaging the sample from different angles. Volumes from each view are then merged to create an improved comprehensive representation of the sample. In a typical multiview approach, the sample is imaged in a stack and re-imaged after an angular rotation in a new stack and so forth until the desired number of views are acquired. To reduce striping artifacts, it is required to capture a sufficient number of



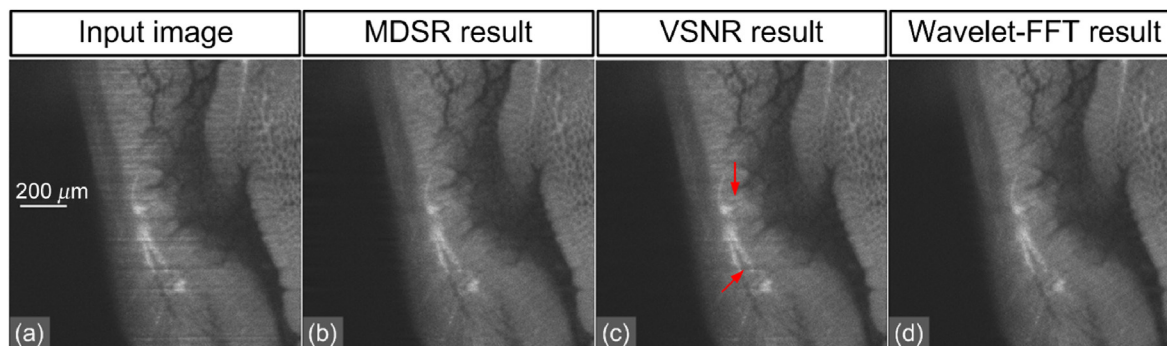


**Fig. 5.** Destriping results on a unidirectional LSM image of the colon: (a) input LSM image, (b) MDSR<sup>90</sup>, (c) VSNR<sup>88</sup>, and (d) wavelet-FFT<sup>80</sup> results. Reprinted with permission from (Liang et al., 2016): Xiao Liang, Yali Zang, Di Dong, Liwen Zhang, Mengjie Fang, Xin Yang, Alicia Arranz, Jorge Ripoll, Hui Hui, Jie Tian, “Stripe artifact elimination based on nonsubsampling contourlet transform for light-sheet fluorescence microscopy,” *J. Biomed. Opt.* 21(10) 106005 (October 26, 2016), © 2016 Society of Photo-Optical Instrumentation Engineers (SPIE).

angles to achieve full coverage of the sample with significant overlap. Afterwards, all optical sections are usually merged using dedicated fusion and deconvolution algorithms to combine the images in a high-resolution volume with improved SBR (Preibisch et al., 2010). It is worth noting that in multiview approaches striping effects could be present in every single optical section, but they will be oriented differently, impacting distinct areas. Consequently, fusing the views with local weights based on an image quality metric allows to greatly reduce the presence of the artifacts in the merged volume. Furthermore, even if multiview imaging does not guarantee an entirely uniform illumination (for example within the centre of thick samples), the overall merged image quality is greatly enhanced compared to single view methods (Guo et al., 2020). The comparison, reported by Swoger et al. and shown in Fig. 6, between a single-view and a fused multi-view one-photon LSM acquisition of a Medaka embryo is a representative example of such improvement and of striping suppression.

Lastly, if rotation is not mandatory, or the sample requires a horizontal orientation, such as plated cells or brain slices, light-sheet illumination can also be implemented in different arrangements (Wu et al., 2011). Although multiview improves the image quality and reduces stripes artifacts, it suffers from two main drawbacks: limitation in the acquisition rate and photobleaching. Indeed, rotating the specimen can be quite problematic due to the slow rotation speed of stage motors and the volume of the sample is cumulatively exposed to illumination light for several times longer than with single-view acquisition. Thus, multiview is more suitable for high-quality imaging of fixed samples or of slowly evolving systems. An alternative devoid of these limitations and still capable of reducing the striping in LSM is adding to the common single illumination objective a second counter-facing objective with a specular optical excitation pathway (also called multi-arm approach), as represented in Fig. 2g. The introduction of a second objective allows to image consecutively or simultaneously the same plane using illumination from two opposite directions, filling-in missing information and preventing single-side shadows (de Vito et al., 2020b; Ding et al., 2013; Medeiros et al., 2015; Tomer et al., 2012; Wu et al., 2013, 2016). The image of the plane is obtained either by computationally fusing the two single-side images or directly without further processing.

Another hybrid solution was reported by Dong et al. (2014) where a two-step procedure is introduced to simultaneously solve two kinds of stripes artifacts. The first part regards the possibility of removing motionless stripes, which do not move together with a displacing sample, originated by inhomogeneous illumination or impurities present outside the sample. As schematically represented in Fig. 2h, this method consists in vertically scanning

the sample, while it is translated continuously during the image acquisition process; the overlapping images are then merged into a single one. However, to suppress classical “non-moving” stripes they applied the VSNR algorithm (Fehrenbach et al., 2012) already mentioned in the previous section.

The multidirectional, multi-arm or multiview optical approaches, where the striping artifacts are reduced by illuminating the sample or by detecting light from different directions, become ineffective when complex and extended spatial distributions of absorbing materials are present inside the sample. A possible solution for this challenge is represented by combining mSPIM (and straightforwardly multi-sided illumination and multiview imaging) with optical projection tomography (OPT). Although the compatibility of the two imaging modalities in a single hybrid system has already been proven by performing multichannel imaging on fixed samples (Gualda et al., 2013; Mayer et al., 2014) and in live zebrafish embryos (Bassi et al., 2015), in a recent work Mayer et al. (2018) explored a synergistic relationship by using one modality to improve the other, computationally correcting the artifacts in LSM. In their hybrid method, called OPTiSPIM, they combined the information provided by a series of projection images of the sample collected from different angles, to quantify the attenuation due to the shadowing in SPIM acquisitions. In particular, measuring the 3D attenuation map and applying an algebraic reconstruction algorithm, they calculate the corrections via a path integral over attenuation coefficient values along the illumination and detection path. The method has been successfully tested with a cleared embryonic mouse head, even if some residual shadow artifacts can persist after the correction application, especially when the attenuation is too strong (i.e. when the signal is reduced to background levels).

## 5. Discussion and conclusions

Light-sheet fluorescence microscopy is a planar illumination technique that provided a revolutionary contribution to optical imaging of biological specimens. However, image quality degrades in presence of striping artifacts, correlated to the side illumination and originating during light propagation in samples containing scattering or absorbing structures. In this review, we presented and discussed the up-to-date methods adopted in LSM to remove striping artifacts, distinguishing between purely optical approaches, digital post-processing image elaboration algorithms and hybrid methods which combine both, as summarized in Table 1.

A quantitative and comparative analysis of the different techniques and methodologies has not yet been carried out. The first hindrance to a direct comparison between them is certainly on the

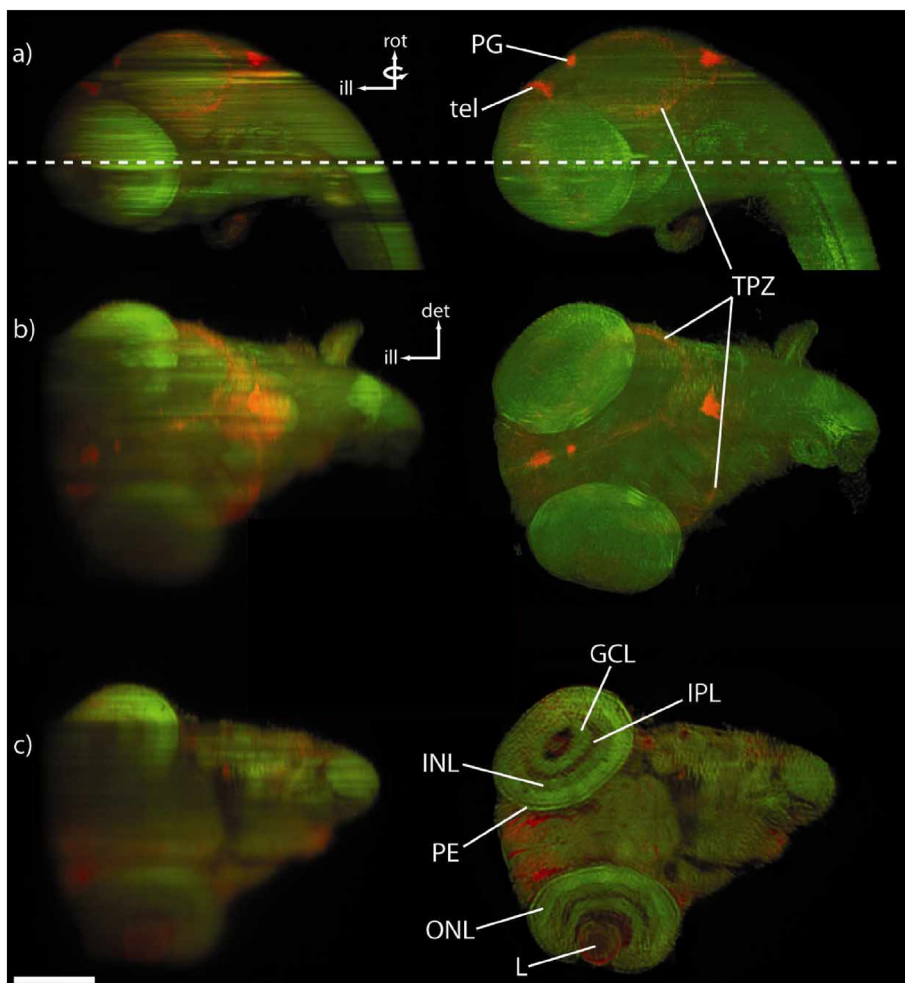


**Fig. 6.** Medaka embryo, stage 32, nuclear label (green) and Mcf0001MGR-1G19bd1 in situ hybridization (red). Left: single-view images; right: 6-view fusion using the MVD-MAPGG algorithm. Striping reduction is clearly visible. (a,b) Maximum-value projections along orthogonal axes. (c) Slice at the depth indicated by the dashed line in (a). Internal structures such as the lens (L), pigmented epithelium (PE), ganglion cell layer (GCL), outer (ONL) and inner nuclear layers (INL), and the inner plexiform layer (IPL) of the retina are well-defined in the fusion. The illumination (ill), detection (det), and rotation (rot) axes are indicated for the single-view images. Scale bar = 200  $\mu\text{m}$ . Figure adapted with changes and with permission from (Swoger et al., 2007): Jim Swoger, Peter Verwee, Klaus Greger, Jan Huisken, Ernst H.K. Stelzer, "Multi-view image fusion improves resolution in three-dimensional microscopy," *Opt. Express* 15, 8029–8042 (2007). <https://doi.org/10.1364/OE.15.008029>. © 2007 Optical Society of America.

structural level, since optical designs are often completely different. Moreover, a single arrangement enabling the use of all approaches alternatively or combined is not feasible, simply because some of them cannot coexist.

All the purely optical methods reported in this work grant a direct reduction of striping artifacts without any post-processing, ranging from partial to almost complete suppression. On the other hand, they require specific optical designs and hardware modifications with respect to standard SPIM, ranging from the simple addition of single optical elements (e.g. axicon lens, optical diffuser) in a well-defined position, to the more complex integration of bulky optoelectronic devices, which may be demanding and expensive (e.g. galvo-mirrors, AODs). Alternative excitation techniques do not guarantee striping removal if the artifacts arise along the direction of the detected fluorescence. Although infrared excitation may provide several benefits, as discussed in section 2.4, it is worth noting that adding such capability to a 1P light-sheet microscope would require a complete optical redesign in order to account for the different wavelength band. Thus, infra-red illumination is not practically straightforward, but remains definitely recommended to reduce scattering and light absorption with respect to visible illumination, hence increasing penetration depth

and decreasing striping probability. Partially leaving this all-optical class, the implementation of a multiview based LSFM is optically effortless, essentially asking only for the addition of a sample rotator stage.

Image artifact correction provided by digital elaboration can be applied to any microscopy setup since it can be carried out in post-processing and has been shown to perform competitively with optical methods. Notable is the case of hybrid solutions based on multiview fusion where striping suppression can be achieved concurrently with resolution enhancement and improvement in illumination uniformity. Although the computational power of standard computers and workstations is steadily increasing each year, some of these methods may require state-of-the-art hardware resources to handle and process over a reasonable time frame terabyte-sized dataset, as often produced by LSFM. Their integration in the image processing pipeline may also require significant programming skills, if the algorithms are not directly provided in the form of plugins for image analysis software or as stand-alone executables. Another issue is that sometimes digital processing may not lead to the expected results because of unforeseen differences between the experimental imaging conditions (e.g. tissue scattering and absorption properties) and the models considered

**Table 1**  
Main methods to reduce striping artifacts in LSFM.

| Methods                                 | Benefits   | Limitations/Requirements   | Costs          | Main references   |
|---|--|--|----------------|---|
| <b>All-Optical</b>                      |  |  |                |   |
| <b>Self-reconstructing beams</b>        |  |  |                |   |
| Bessel                                  | -Easy optical implementation<br>-Increase resolution isotropy<br>-In vivo and functional imaging<br>-No post-processing                          | -Reduced SBR and image contrast  | \$             | Fahrbach et al. (2010)<br>Meinert et al. (2016)<br>Müllenbroich et al., 2018                  |
| Airy                                    | -High penetration depth<br>-High contrast<br>-In vivo and functional imaging   | -SLM for phase modulation<br>-Post-processing deconvolution required   | \$\$           | Kafian et al. (2020)  |
| <b>Multidirectional illumination</b>    |  |  |                |   |
| Beam pivoting                           | -In vivo and functional imaging<br>-No post-processing   | -Bulky and expensive scanning head<br>-AOD or resonant galvos for improved striping attenuation and fast process imaging                                   | \$ to \$\$     | Huisken and Stainier (2007)<br>Sancataldo et al. (2019)                                       |
| DSLMS beam pivoting                     | -In vivo and functional imaging<br>-Adaptable to confocal detection<br>-No post-processing   | -Bulky and expensive scanning head<br>-AOD or resonant galvos for improved striping attenuation and fast process imaging                                   | \$\$           | Glaser et al. (2018)<br>Ricci et al. (2020)   |
| <b>DSLMS variants</b>                   |  |  |                |   |
| DSLMS                                   | -Adaptable to confocal detection<br>-No additional optics<br>-No post-processing   | -Bulky and expensive scanning head   | \$\$           | Pampaloni et al. (2011)   |
| Axially dithered DSLMS                  | -Adaptable to confocal detection<br>-No post-processing  | -Bulky and expensive scanning head<br>-Slight artifacts reduction  | \$\$           | Liu et al. (2019)   |
| Diagonally swept DSLMS                  | -Large angular diversity<br>-No post-processing  | -Proper sample mounting<br>-Bulky and expensive scanning head  | \$\$           | Dean et al. (2016)  |
| Diffuse DSLMS                           | Easy optical implementation  | -Low imaging quality without pivoting<br>-Hardly adaptable to confocal detection   | \$             | Taylor et al. (2018)  |
| <b>Light coherence controlled</b>       |  |  |                |   |
| Coded light-sheet array microscopy CLAM | No mechanical scanning   | -Angle-misaligned mirrors<br>-Resolution affected<br>-Careful optical design   | \$\$           | Ren et al. (2020)   |
| Incoherent source                       | -No laser source required<br>-low cost   | -Complex alignment<br>-Sample specific parameter optimization  | \$             | Calisesi et al. (2019)  |
| Spatio-temporal coherence controlled    | Artifacts attenuation by light coherence deterioration   | -Supercontinuum fibre laser implementation<br>-Limited pivoting dynamics   | \$\$\$         | Merino et al., 2015<br>Di Battista et al. (2019)  |
| <b>NIR illumination</b>                 |  |  |                |   |
| Near infrared II window                 | -Reduced excitation scattering and absorption<br>-Reduced photo-toxicity<br>-Improved imaging depth<br>-Animal visual organs not photostimulated | -Careful optical design<br>-Requires powerful pulsed laser sources for two-photon excitation<br>-Affected by pulse dispersion                              | \$\$\$         | Wang et al. (2019)  |
| <b>Others</b>                           |  |  |                |   |
| Elliptical holographic diffuser         | No speckle pattern   | Hardly adaptable to confocal detection   | \$\$           | Salili et al. (2018)  |
| <b>Digital</b>                          |  |  |                |   |
| Physical model-based                    | -No extra hardware/imaging acquisitions<br>-Improved quality and resolution<br>-Compensation of illumination inhomogeneity                       | -Computational post-processing<br>-Model dependent performance and robustness<br>-Risk of residual artifacts due to model limitations                      | \$             | Uddin et al. (2011)   |
| Non-linear smoothing                    | -No extra optical hardware<br>-Improved quality and resolution<br>-Compensation of illumination inhomogeneity                                    | -Manual parameter tweaking<br>-Residual artifacts present<br>-Hardly adaptable to real time measurements   | \$             | Leischner et al. (2010)<br>Ding et al. (2013)<br>Pollatou (2020)                              |
| Wavelet-Fourier filtering               | -No extra optical hardware<br>-Improved quality and resolution<br>-Fast computation<br>-Easy implementation                                      | -Not effective with strong attenuation<br>-Introduces blurring<br>-Hardly adaptable to real time measurements  | \$             | Münch et al. (2009)   |
| MDSR                                    | -No extra optical hardware<br>-Improved quality and resolution<br>-No blurring   | - Heavy computational load<br>-Hardly adaptable to real time measurements  | \$\$           | Liang et al. (2016)   |
| Variational, VSNR                       | -No extra optical hardware<br>-Improved quality and resolution   | -Heavy computational load<br>-Residual artifacts present<br>-Hardly adaptable to real time measurements  | \$\$           | Fehrenbach et al. (2012)<br>Chang et al. (2013) Escande et al. (2017)                         |
| <b>Hybrid</b>                           |  |  |                |   |
| Multiview fusion                        | -Improved resolution and SBR<br>-High quality imaging  | -Long acquisition time for sequential acquisitions<br>-Increased photobleaching<br>-Hardly feasible for fast biological processes<br>-Sample rotator stage | \$\$ to \$\$\$ | Preibisch et al. (2010)<br>Tomer et al. (2012)<br>Medeiros et al. (2015)<br>Guo et al. (2020) |
| Dual-side illumination                  | -High data acquisition rate<br>-Improved quality and illumination uniformity   | -Complex alignment<br>-Doubling of the excitation beam path elements   | \$\$ to \$\$\$ | Huisken and Stainier (2007)   |
| Vertical scanned + VSNR                 | Removes motionless stripes   |  | \$\$           | Dong et al. (2014)  |

Table 1 (continued)

| Methods  | Benefits   | Limitations/Requirements   | Costs | Main references     |
|----------|--|--|-------|---------------------|
| OPTiSPIM | -Reduced artifacts in unavoidable absorbing regions<br>-Compatible with live imaging | -Translational stage<br>-Computational post-processing<br>Extended depth of field required for small samples | \$\$  | Mayer et al. (2018) |

within the algorithms. Moreover, these methods, in extreme cases or when the detected signal becomes comparable or lower than the background noise level, could even introduce reconstruction artifacts themselves.

The choice of the method to employ in a light-sheet microscope to improve image quality via striping artifact reduction should be guided by the biological scope of the research performed with the instrument, since there is no single approach that performs best without any limitation.

Imaging and over-time tracking of dynamic or fast in-vivo biological processes requires approaches that do not impair the measurement rate and cause increased photobleaching. In this regard, Bessel beam and multidirectional illumination methods are suitable to record sample activity and reconstruct functional maps, while lessening striping. Computational techniques can be also applied in such experiments, if the risk of introducing artifacts is negligible and if the post-processing period does not cause experimental dead times or a counterproductive delay in the analysis and follow-up studies. Analogously, multiview implementations present limitations in terms of acquisition rate and photobleaching, making them unfit for fast dynamic experiments or imaging of live animals. On the other hand, they are perfectly suitable approaches for imaging slowly evolving systems or obtaining structural reconstructions of fixed ex-vivo samples. The final outcome, after volume stitching, deconvolution and fusion, shows an overall improved quality, higher resolution, better illumination uniformity and reduced striping artifacts. Finally, using different illumination wavelengths, e.g. infrared excitation, for biological applications is particularly convenient when dealing with animal photostimulation. Multiphoton illumination avoids stimulating the animal visual organs while performing functional imaging, whereas one-photon excitation in the visible spectrum may cause undesired reactions, requiring complex excitation geometries to mitigate this issue.

In conclusion, this review aims to present all currently available approaches to mitigate or remove striping artifacts from images acquired by LSFM. By discussing their advantages, limitations and technical requirements, it should facilitate the choice of the most suitable method for each biological study of interest.

## Funding

This project has received funding from the European Union's Horizon 2020 research and innovation Framework Programme under grant agreements No. 720270 (HBP-SGA1), 785907 (HBP-SGA2), 945539 (HBP-SGA3), and 871124 (Laserlab-Europe), and from the EU program H2020 EXCELLENT SCIENCE - European Research Council (ERC) under grant agreement n. 692943 (BrainBIT). This research has also been supported by the Advanced Lightsheet Microscopy Italian Mode of Euro-Bioimaging ERIC, by Progetto ordinario di Ricerca Finalizzata del Ministero della salute RF-2013-02355240 and by "Ente Cassa di Risparmio di Firenze" (private foundation). GS is funded by PON AIM 1809078–1. VG and MCM are funded each by a Marie Skłodowska-Curie fellowship (MSCA-IF-EF-ST "MesoBrainMicr" and "Optoheart", grant agreements No. 793849 and 842893, respectively).

## Disclosures

The authors declare that there are no conflicts of interest related to this paper.

## Author statement

All authors certify that they have participated sufficiently in the work to take public responsibility for the content, including participation in the concept, design, analysis, writing, or revision of the manuscript.

## References

- Bassi, A., Schmid, B., Huisken, J., 2015. Optical tomography complements light sheet microscopy for in toto imaging of zebrafish development. *Dev* 142, 1016–1020. <https://doi.org/10.1242/dev.116970>.
- Baumgart, E., Kubitscheck, U., 2012. Scanned light sheet microscopy with confocal slit detection. *Opt Express* 20, 21805. <https://doi.org/10.1364/oe.20.021805>.
- Calisesi, G., Castriotta, M., Candeo, A., Pistocchi, A., D'Andrea, C., Valentini, G., Farina, A., Bassi, A., 2019. Spatially modulated illumination allows for light sheet fluorescence microscopy with an incoherent source and compressive sensing. *Biomed. Opt Express* 10, 5776. <https://doi.org/10.1364/boe.10.005776>.
- Cella Zanacchi, F., Lavagnino, Z., Pesce, M., Difato, F., Ronzitti, E., Diaspro, A., 2011. Two-photon fluorescence excitation within a light sheet based microscopy architecture. *Multiphot. Microsc. Biomed. Sci.* XI 7903, 79032W. <https://doi.org/10.1117/12.879792>.
- Chang, Y., Fang, H., Yan, L., Liu, H., 2013. Robust destriping method with unidirectional total variation and framelet regularization. *Opt Express* 21, 23307. <https://doi.org/10.1364/oe.21.023307>.
- Chatterjee, K., Pratiwi, F.W., Wu, F.C.M., Chen, P., Chen, B.C., 2018. Recent progress in light sheet microscopy for biological applications. *Appl. Spectrosc.* 72, 1137–1169. <https://doi.org/10.1177/0003702818778851>.
- Chen, S.W.W., Pellequer, J.L., 2011. DeStripe: frequency-based algorithm for removing stripe noises from AFM images. *BMC Struct. Biol.* 11 <https://doi.org/10.1186/1472-6807-11-7>.
- Costa, A., Candeo, A., Fieramonti, L., Valentini, G., Bassi, A., 2013. Calcium dynamics in root cells of *Arabidopsis thaliana* visualized with selective plane illumination microscopy. *PLoS One* 8. <https://doi.org/10.1371/journal.pone.0075646>.
- Costantini, I., Ghobril, J.P., Di Giovanna, A.P., Allegra Mascaro, A.L., Silvestri, L., Müllenbroich, M.C., Onofri, L., Conti, V., Vanzi, F., Sacconi, L., Guerrini, R., Markram, H., Iannello, G., Pavone, F.S., 2015. A versatile clearing agent for multimodal brain imaging. *Sci. Rep.* 5, 1–9. <https://doi.org/10.1038/srep09808>.
- Daetwyler, S., Huisken, J., 2016. Fast fluorescence microscopy with light sheets. *Biol. Bull.* 231, 14–25. <https://doi.org/10.1086/689588>.
- de Vito, G., Fornetto, C., Ricci, P., Müllenbroich, C., Sancataldo, G., Turrini, L., Mazzamuto, G., Tiso, N., Sacconi, L., Fanelli, D., Silvestri, L., Vanzi, F., Pavone, F.S., 2020a. Two-photon High-Speed Light-Sheet Volumetric Imaging of Brain Activity during Sleep in Zebrafish Larvae 1122604, p. 3. <https://doi.org/10.1117/12.2542285>.
- de Vito, G., Ricci, P., Turrini, L., Tiso, N., Vanzi, F., Silvestri, L., Pavone, F.S., 2020b. Effects of excitation light polarization on fluorescence emission in two-photon light-sheet microscopy. *Biomed. Opt. Express* 11, 4651. <https://doi.org/10.1364/boe.396388>.
- de Vito, G., Turrini, L., Fornetto, C., Ricci, P., Müllenbroich, C., Sancataldo, G., Trabalzini, E., Mazzamuto, G., Tiso, N., Sacconi, L., Fanelli, D., Silvestri, L., Vanzi, F., Pavone, F.S., 2020c. Two-photon Light-Sheet Microscopy for High-Speed Whole-Brain Functional Imaging of Zebrafish Neuronal Physiology and Pathology 1136004, vol. 3. <https://doi.org/10.1117/12.2560341>.
- Dean, K.M., Roudot, P., Reis, C.R., Wolf, E.S., Mettlen, M., Fiolka, R., 2016. Diagonally scanned light-sheet microscopy for fast volumetric imaging of adherent cells. *Biophys. J.* 110, 1456–1465. <https://doi.org/10.1016/j.bpj.2016.01.029>.
- Di Battista, D., Merino, D., Zacharakis, G., Loza-Alvarez, P., Olarte, O.E., 2019. Enhanced light sheet elastic scattering microscopy by using a supercontinuum laser. *Methods Protoc* 2, 1–12. <https://doi.org/10.3390/mps2030057>.
- Ding, W., Li, A., Wu, J., Yang, Z., Meng, Y., Wang, S., Gong, H., 2013. Automatic macroscopic density artefact removal in a Nissl-stained microscopic atlas of whole mouse brain. *J. Microsc.* 251, 168–177. <https://doi.org/10.1111/jmi.12058>.
- Ding, Z., Ren, H., Zhao, Y., Nelson, J.S., Chen, Z., 2002. High-resolution optical

- coherence tomography over a large depth range with an axicon lens. *Opt. Lett.* 27, 243. <https://doi.org/10.1364/ol.27.00243>.
- Dodt, H.U., Leischner, U., Schierloh, A., Jähring, N., Mauch, C.P., Deininger, K., Deussing, J.M., Eder, M., Zieglgänsberger, W., Becker, K., 2007. Ultramicroscopy: three-dimensional visualization of neuronal networks in the whole mouse brain. *Nat. Methods* 4, 331–336. <https://doi.org/10.1038/nmeth1036>.
- Dong, D., Arranz, A., Zhu, S., Yang, Y., Shi, L., Wang, J., Shen, C., Tian, J., Ripoll, J., 2014. Vertically scanned laser sheet microscopy. *J. Biomed. Opt.* 19, 1. <https://doi.org/10.1117/1.jbo.19.10.106001>.
- Dougherty Edward, R., 1992. *An Introduction to Morphological Image Processing*. SPIE.
- Duocastella, M., Sancataldo, G., Saggau, P., Ramoino, P., Bianchini, P., Diaspro, A., 2017. Fast inertia-free volumetric light-sheet microscope. *ACS Photonics* 4, 1797–1804. <https://doi.org/10.1021/acsphotonics.7b00382>.
- Durnin, J., Miceli, J., Eberly, J.H., 1987. Diffraction-free beams. *Phys. Rev. Lett.* 58, 1499–1501. <https://doi.org/10.1103/PhysRevLett.58.1499>.
- Engelbrecht, C.J., Stelzer, E.H., 2006. Resolution enhancement in a light-sheet-based microscope (SPIM). *Opt. Lett.* 31, 1477. <https://doi.org/10.1364/ol.31.001477>.
- Escande, P., Weiss, P., Zhang, W., 2017. A variational model for multiplicative structured noise removal. *J. Math. Imag. Vis.* 57, 43–55. <https://doi.org/10.1007/s10851-016-0667-3>.
- Escobet-Montalbán, A., Gasparoli, F.M., Nylk, J., Liu, P., Yang, Z., Dholakia, K., 2018. Three-photon light-sheet fluorescence microscopy. *Opt. Lett.* 43, 5484. <https://doi.org/10.1364/ol.43.005484>.
- Fahrbaach, F.O., Gurchenkov, V., Alessandri, K., Nassoy, P., Rohrbach, A., 2013a. Light-sheet microscopy in thick media using scanned Bessel beams and two-photon fluorescence excitation. *Opt. Express* 21, 13824. <https://doi.org/10.1364/oe.21.013824>.
- Fahrbaach, F.O., Gurchenkov, V., Alessandri, K., Nassoy, P., Rohrbach, A., 2013b. Self-reconstructing sectioned Bessel beams offer submicron optical sectioning for large fields of view in light-sheet microscopy. *Opt. Express* 21, 11425. <https://doi.org/10.1364/oe.21.011425>.
- Fahrbaach, F.O., Rohrbach, A., 2012. Propagation stability of self-reconstructing Bessel beams enables contrast-enhanced imaging in thick media. *Nat. Commun.* 3 <https://doi.org/10.1038/ncomms1646>.
- Fahrbaach, F.O., Simon, P., Rohrbach, A., 2010. Microscopy with self-reconstructing beams. *Nat. Photonics* 4, 780–785. <https://doi.org/10.1038/nphoton.2010.204>.
- Fahrbaach, F.O., Voigt, F.F., Schmid, B., Helmchen, F., Huisken, J., 2013c. Rapid 3D light-sheet microscopy with a tunable lens. *Opt. Express* 21, 21010. <https://doi.org/10.1364/oe.21.021010>.
- Fehrenbach, J., Weiss, P., Lorenzo, C., 2012. Variational algorithms to remove stationary noise: applications to microscopy imaging. *IEEE Trans. Image Process.* 21, 4420–4430. <https://doi.org/10.1109/TIP.2012.2206037>.
- Gadallah, F.L., Csilag, F., Smith, E.J.M., 2000. Destriping multisensor imagery with moment matching. *Int. J. Rem. Sens.* 21, 2505–2511. <https://doi.org/10.1080/01431160050030592>.
- Garcés-Chávez, V., McGloin, D., Melville, H., Sibbett, W., Dholakia, K., 2002. Simultaneous micromanipulation in multiple planes using a self-reconstructing light beam. *Nature* 419, 145–147. <https://doi.org/10.1038/nature01007>.
- Gavryusev, V., Sancataldo, G., Ricci, P., Montalbano, A., Fornetto, C., Turrini, L., Laurino, A., Pesce, L., de Vito, G., Tiso, N., Vanzi, F., Silvestri, L., Pavone, F.S., 2019. Dual-beam confocal light-sheet microscopy via flexible acousto-optic deflector. *J. Biomed. Opt.* 24, 1. <https://doi.org/10.1117/1.jbo.24.10.106504>.
- Girkin, J.M., Carvalho, M.T., 2018. The light-sheet microscopy revolution. *J. Opt.* 20 <https://doi.org/10.1088/2040-8986/aab58a>.
- Glaser, A.K., Chen, Y., Yin, C., Wei, L., Barner, L.A., Reder, N.P., Liu, J.T.C., 2018. Multidirectional digital scanned light-sheet microscopy enables uniform fluorescence excitation and contrast-enhanced imaging. *Sci. Rep.* 8, 2–12. <https://doi.org/10.1038/s41598-018-32367-5>.
- Gualda, E.J., Vale, T., Almada, P., Feijó, J.A., Martins, G.G., Moreno, N., 2013. OpenSpinMicroscopy: an open-source integrated microscopy platform. *Nat. Methods* 10, 599–600. <https://doi.org/10.1038/nmeth.2508>.
- Guo, M., Li, Y., Su, Y., Lambert, T., Nogue, D.D., Moyle, M.W., Duncan, L.H., Ikegami, R., Santella, A., Rey-Suarez, I., Green, D., Beiriger, A., Chen, J., Vishwasrao, H., Ganesan, S., Prince, V., Waters, J.C., Annunziata, C.M., Hafner, M., Mohler, W.A., Chitnis, A.B., Upadhyaya, A., Usdin, T.B., Bao, Z., Colón-Ramos, D., La Riviere, P., Liu, H., Wu, Y., Shroff, H., 2020. Rapid image deconvolution and multiview fusion for optical microscopy. *Nat. Biotechnol.* 38, 1337–1346. <https://doi.org/10.1038/s41587-020-0560-x>.
- Herman, R.M., Wiggins, T.A., 1991. Production and uses of diffractionless beams. *J. Opt. Soc. Am. A* 8, 932. <https://doi.org/10.1364/josaa.8.000932>.
- Huisken, J., Stainier, D.Y.R., 2007. Even fluorescence excitation by multidirectional selective plane illumination microscopy (mSPIM). *Opt. Lett.* 32, 2608. <https://doi.org/10.1364/ol.32.002608>.
- Huisken, J., Swoger, J., Del Bene, F., Wittbrodt, J., Stelzer, E.H.K., 2004. Optical sectioning deep inside live embryos by selective plane illumination microscopy. *Science* 80, 1007–1009. <https://doi.org/10.1126/science.1100035>.
- Jemielita, M., Taormina, M.J., Delaurier, A., Kimmel, C.B., Parthasarathy, R., 2013. Comparing phototoxicity during the development of a zebrafish craniofacial bone using confocal and light sheet fluorescence microscopy techniques. *J. Biophot.* 6, 920–928. <https://doi.org/10.1002/jbio.201200144>.
- Kafian, H., Lalenejad, M., Moradi-Mehr, S., Birgani, S.A., Abdollahpour, D., 2020. Light-sheet fluorescence microscopy with scanning non-diffracting beams. *Sci. Rep.* 10, 1–12. <https://doi.org/10.1038/s41598-020-63847-2>.
- Keller, P.J., Ahrens, M.B., 2015. Visualizing whole-brain activity and development at the single-cell level using light-sheet microscopy. *Neuron* 85, 462–483. <https://doi.org/10.1016/j.neuron.2014.12.039>.
- Keller, P.J., Ahrens, M.B., Freeman, J., 2014. Light-sheet imaging for systems neuroscience. *Nat. Methods* 12, 27–29. <https://doi.org/10.1038/nmeth.3214>.
- Keller, P.J., Dodt, H.U., 2012. Light sheet microscopy of living or cleared specimens. *Curr. Opin. Neurobiol.* 22, 138–143. <https://doi.org/10.1016/j.conb.2011.08.003>.
- Keller, P.J., Schmidt, A.D., Wittbrodt, J., Stelzer, E.H.K., 2008. Reconstruction of zebrafish early embryonic development by scanned light sheet microscopy. *Science* (80- 322), 1065–1069. <https://doi.org/10.1126/science.1162493>.
- Krull, A., Vičar, T., Prakash, M., Lalit, M., Jug, F., 2020. Probabilistic Noise2Void: Unsupervised Content-Aware Denoising. *Front. Comput. Sci.* 0, 5. <https://doi.org/10.3389/FCOMP.2020.00005>.
- Lavagnino, Z., Cella Zanacchi, F., Ronzitti, E., Diaspro, A., 2013. Two-photon excitation selective plane illumination microscopy (2PE-SPIM) of highly scattering samples: characterization and application. *Opt. Express* 21, 5998. <https://doi.org/10.1364/oe.21.005998>.
- Lavagnino, Z., Sancataldo, G., D'Amora, M., Follert, P., De Pietri Tonelli, D., Diaspro, A., Cella Zanacchi, F., 2016. 4D (x-y-z-t) imaging of thick biological samples by means of Two-Photon Inverted Selective Plane Illumination Microscopy (2PE-iSPIM). *Sci. Rep.* 6, 1–9. <https://doi.org/10.1038/srep23923>.
- Leischner, U., Schierloh, A., Zieglgänsberger, W., Dodt, H.U., 2010. Formalin-induced fluorescence reveals cell shape and morphology in biological tissue samples. *PLoS One* 5. <https://doi.org/10.1371/journal.pone.0010391>.
- Lemon, W.C., Pulver, S.R., Höckendorf, B., McDole, K., Branson, K., Freeman, J., Keller, P.J., 2015. Whole-central nervous system functional imaging in larval *Drosophila*. *Nat. Commun.* 6 <https://doi.org/10.1038/ncomms8924>.
- Liang, X., Zang, Y., Dong, D., Zhang, L., Fang, M., Yang, X., Arranz, A., Ripoll, J., Hui, H., Tian, J., 2016. Stripe artifact elimination based on nonsubsampled contourlet transform for light sheet fluorescence microscopy. *J. Biomed. Opt.* 21, 106005. <https://doi.org/10.1117/1.jbo.21.10.106005>.
- Liu, Y., Lauderdale, J.D., Kner, P., 2019. Stripe artifact reduction for digital scanned structured illumination light sheet microscopy. *Opt. Lett.* 44, 2510. <https://doi.org/10.1364/ol.44.002510>.
- Mandrachia, B., Hua, X., Guo, C., Son, J., Urner, T., Jia, S., 2020. Fast and accurate sCMOS noise correction for fluorescence microscopy. *Nat. Commun.* 11, 1–12. <https://doi.org/10.1038/s41467-019-13841-8>.
- Mayer, J., Robert-Moreno, A., Danuser, R., Stein, J.V., Sharpe, J., Swoger, J., 2014. OPTiSPIM: integrating optical projection tomography in light sheet microscopy extends specimen characterization to nonfluorescent contrasts. *Opt. Lett.* 39, 1053. <https://doi.org/10.1364/ol.39.001053>.
- Mayer, J., Robert-Moreno, A., Sharpe, J., Swoger, J., 2018. Attenuation artifacts in light sheet fluorescence microscopy corrected by OPTiSPIM. *Light Sci. Appl.* 7 <https://doi.org/10.1038/s41377-018-0068-z>.
- McGloin, D., Dholakia, K., 2005. Bessel beams: diffraction in a new light. *Contemp. Phys.* 46, 15–28. <https://doi.org/10.1080/0010751042000275259>.
- Medeiros, G. de, Norlin, N., Gunther, S., Albert, M., Panavaite, L., Fiuza, U.M., Peri, F., Hiriagi, T., Krzic, U., Huftagel, L., 2015. Confocal multiview light-sheet microscopy. *Nat. Commun.* 6, 1–8. <https://doi.org/10.1038/ncomms9881>.
- Meinert, T., Tietz, O., Palme, K.J., Rohrbach, A., 2016. Separation of ballistic and diffusive fluorescence photons in confocal Light-Sheet Microscopy of Arabidopsis roots. *Sci. Rep.* 6, 1–14. <https://doi.org/10.1038/srep30378>.
- Merino, D., Olarte, O., Cruz, J.L., Díez, A., Barmenkov, Y.O., Andrés, M.V., Pérez-Millán, P., Loza-Alvarez, P., 2015. Use of a supercontinuum laser source with low temporal coherence for elastic scattering light sheet microscopy. In: *Proceedings 2015 European Conference on Lasers and Electro-Optics - European Quantum Electronics Conference. CLEO/Europe-EQEC*.
- Mickelait, M., Schmid, B., Weber, M., Fahrbaach, F.O., Hombach, S., Reischauer, S., Huisken, J., 2014. High-resolution reconstruction of the beating zebrafish heart. *Nat. Methods* 11, 919–922. <https://doi.org/10.1038/nmeth.3037>.
- Müllenbroich, M.C., Silvestri, L., Di Giovanna, A.P., Mazzamuto, G., Costantini, I., Sacconi, L., Pavone, F.S., 2018a. High-fidelity imaging in brain-wide structural studies using light-sheet microscopy. *eNeuro* 5. <https://doi.org/10.1523/ENEURO.0124-18.2018>.
- Müllenbroich, M.C., Silvestri, L., Onofri, L., Costantini, I., Hoff, M. van't, Sacconi, L., Iannello, G., Pavone, F.S., 2015. Comprehensive optical and data management infrastructure for high-throughput light-sheet microscopy of whole mouse brains. *Neurophotonics* 2, 041404. <https://doi.org/10.1117/1.nph.2.4.041404>.
- Müllenbroich, M.C., Turrini, L., Silvestri, L., Alterlini, T., Gheisari, A., Vanzi, F., Sacconi, L., Pavone, F.S., 2018b. Bessel beam illumination reduces random and systematic errors in quantitative functional studies using light-sheet microscopy. *Front. Cell. Neurosci.* 12, 1–12. <https://doi.org/10.3389/fncel.2018.00315>.
- Münc, B., Trtik, P., Marone, F., Stapanioni, M., 2009. Stripe and ring artifact removal with combined wavelet-Fourier filtering. *EMPA Act* 17, 34–35. <https://doi.org/10.1364/oe.17.008567>.
- Palero, J., Santos, S.I.C.O., Artigas, D., Loza-Alvarez, P., 2010. A simple scanless two-photon fluorescence microscope using selective plane illumination. *Opt. Express* 18, 8491. <https://doi.org/10.1364/oe.18.008491>.
- Pampaloni, F., Ansari, N., Girard, P., Stelzer, E.H.K., 2011. Light sheet-based fluorescence microscopy (LSFM) reduces phototoxic effects and provides new means for the modern life sciences. *Opt. InfoBase Conf. Pap.* 8086, 1–6. <https://doi.org/10.1117/12.889443>.
- Panier, T., Romano, S.A., Olive, R., Pietri, T., Sumbre, G., Candelier, R., Debrégeas, G., 2013. Fast functional imaging of multiple brain regions in intact zebrafish larvae using selective plane illumination microscopy. *Front. Neural Circ.* 7, 1–11. <https://doi.org/10.3389/fncir.2013.00065>.

- Peng, T., Thorn, K., Schroeder, T., Wang, L., Theis, F.J., Marr, C., Navab, N., 2017. A BaSiC tool for background and shading correction of optical microscopy images. *Nat. Commun.* 8, 1–7. <https://doi.org/10.1038/ncomms14836>.
- Pollatou, A., 2020. An automated method for removal of striping artifacts in fluorescent whole-slide microscopy. *J. Neurosci. Methods* 341, 108781. <https://doi.org/10.1016/j.jneumeth.2020.108781>.
- Power, R.M., Huisken, J., 2017. A guide to light-sheet fluorescence microscopy for multiscale imaging. *Nat. Methods* 14, 360–373. <https://doi.org/10.1038/nmeth.4224>.
- Preibisch, S., Saalfeld, S., Schindelin, J., Tomancak, P., 2010. Software for bead-based registration of selective plane illumination microscopy data. *Nat. Methods* 7, 418–419. <https://doi.org/10.1038/nmeth0610-418>.
- Rakwatin, P., Takeuchi, W., Yasuoka, Y., 2007. Stripe noise reduction in MODIS data by combining histogram matching with facet filter. *IEEE Trans. Geosci. Rem. Sens.* 45, 1844–1855. <https://doi.org/10.1109/TGRS.2007.895841>.
- Ren, Y.X., Wu, J., Lai, Q.T.K., Lai, H.M., Siu, D.M.D., Wu, W., Wong, K.K.Y., Tsia, K.K., 2020. Parallelized volumetric fluorescence microscopy with a reconfigurable coded incoherent light-sheet array. *Light Sci. Appl.* 9 <https://doi.org/10.1038/s41377-020-0245-8>.
- Ricci, P., Sancataldo, G., Gavryusev, V., Franceschini, A., Müllenbroich, M.C., Silvestri, L., Pavone, F.S., 2020. Fast multi-directional DSLM for confocal detection without striping artifacts. *Biomed. Opt. Express* 11, 3111. <https://doi.org/10.1364/boe.390916>.
- Rohrbach, A., 2009. Artifacts resulting from imaging in scattering media: a theoretical prediction. *Opt. Lett.* 34, 3041. <https://doi.org/10.1364/ol.34.003041>.
- Salili, S.M., Harrington, M., Durian, D.J., 2018. Note: eliminating stripe artifacts in light-sheet fluorescence imaging. *Rev. Sci. Instrum.* 89, 1–4. <https://doi.org/10.1063/1.5016546>.
- Sancataldo, G., Gavryusev, V., de Vito, G., Turrini, L., Locatelli, M., Fornetto, C., Tiso, N., Vanzi, F., Silvestri, L., Pavone, F.S., 2019. Flexible multi-beam light-sheet fluorescence microscope for live imaging without striping artifacts. *Front. Neuroanat.* 13, 1–8. <https://doi.org/10.3389/fnana.2019.00007>.
- Santi, P.A., 2011. Light sheet fluorescence microscopy: a review. *J. Histochem. Cytochem.* 59, 129–138. <https://doi.org/10.1369/0022155410394857>.
- Scherf, N., Huisken, J., 2015. The smart and gentle microscope. *Nat. Biotechnol.* 33, 815–818. <https://doi.org/10.1038/nbt.3310>.
- Shen, H., Zhang, L., 2009. A MAP-based algorithm for destriping and inpainting of remotely sensed images. *IEEE Trans. Geosci. Rem. Sens.* 47, 1492–1502. <https://doi.org/10.1109/TGRS.2008.2005780>.
- Siedentopf, H., Zsigmondy, R., 1903. Über Sichtbarmachung und Größenbestimmung ultramikroskopischer Teilchen. *Ann. Phys.* 4, 1–39.
- Silvestri, L., Bria, A., Sacconi, L., Iannello, G., Pavone, F.S., 2012. Confocal light sheet microscopy: micron-scale neuroanatomy of the entire mouse brain. *Opt. Express* 20, 20582. <https://doi.org/10.1364/oe.20.020582>.
- Silvestri, L., Costantini, I., Sacconi, L., Pavone, F.S., 2016. Clearing of fixed tissue: a review from a microscopist's perspective. *J. Biomed. Opt.* 21, 081205 <https://doi.org/10.1117/1.jbo.21.8.081205>.
- Siviloglou, G.A., Broky, J., Dogariu, A., Christodoulides, D.N., 2008. Self-healing of optical airy beams. *Opt. InfoBase Conf. Pap.* 16, 12880–12891. <https://doi.org/10.1364/fio.2008.fth06>.
- Smith, K., Li, Y., Piccinini, F., Csucs, G., Balazs, C., Bevilacqua, A., Horvath, P., 2015. CIDRE: an illumination-correction method for optical microscopy. *Nat. Methods* 12, 404–406. <https://doi.org/10.1038/nmeth.3323>.
- Sternberg, S.R., 1986. Grayscale morphology. *Comput. Vision. Graph. Image Process* 35, 333–355. [https://doi.org/10.1016/0734-189X\(86\)90004-6](https://doi.org/10.1016/0734-189X(86)90004-6).
- Swoger, J., Verveer, P., Greger, K., Huisken, J., Stelzer, E.H.K., 2007. Multi-view image fusion improves resolution in three-dimensional microscopy. *Opt. Express* 15, 8029. <https://doi.org/10.1364/oe.15.008029>.
- Tainaka, K., Kubota, S.I., Suyama, T.Q., Susaki, E.A., Perrin, D., Ukai-Tadenuma, M., Ukai, H., Ueda, H.R., 2014. Whole-body imaging with single-cell resolution by tissue decolorization. *Cell* 159, 911–924. <https://doi.org/10.1016/j.cell.2014.10.034>.
- Taylor, M.A., Vanwalleghem, G.C., Favre-Bulle, I.A., Scott, E.K., 2018. Diffuse light-sheet microscopy for stripe-free calcium imaging of neural populations. *J. Biophot.* 11, 1–9. <https://doi.org/10.1002/jbio.201800088>.
- Teranikar, T., Messerschmidt, V., Lim, J., Bailey, Z., Chiao, J.C., Cao, H., Liu, J., Lee, J., 2020. Correcting anisotropic intensity in light sheet images using deazing and image morphology. *APL Bioeng.* 4. <https://doi.org/10.1063/1.5144613>.
- Tomer, R., Khairy, K., Amat, F., Keller, P.J., 2012. Quantitative high-speed imaging of entire developing embryos with simultaneous multiview light-sheet microscopy. *Nat. Methods* 9, 755–763. <https://doi.org/10.1038/nmeth.2062>.
- Truong, T.V., Supatto, W., Koos, D.S., Choi, J.M., Fraser, S.E., 2011. Deep and fast live imaging with two-photon scanned light-sheet microscopy. *Nat. Methods* 8, 757–762. <https://doi.org/10.1038/nmeth.1652>.
- Uddin, M.S., Lee, H.K., Preibisch, S., Tomancak, P., 2011. Restoration of uneven illumination in light sheet microscopy images. *Microsc. Microanal.* 17, 607–613. <https://doi.org/10.1017/S1431927611000262>.
- Ueda, H.R., Ertürk, A., Chung, K., Gradinaru, V., Chédotal, A., Tomancak, P., Keller, P.J., 2020. Tissue clearing and its applications in neuroscience. *Nat. Rev. Neurosci.* 21, 61–79. <https://doi.org/10.1038/s41583-019-0250-1>.
- Vettenburg, T., Dalgarno, H.I.C., Nylk, J., Coll-Lladó, C., Ferrier, D.E.K., Čizmar, T., Gunn-Moore, F.J., Dholakia, K., 2014. Light-sheet microscopy using an Airy beam. *Nat. Methods* 11, 541–544. <https://doi.org/10.1038/nmeth.2922>.
- Voie, A.H., Burns, D.H., Spelman, F.A., 1993. *H\_et\_al-1993-Journal\_of\_the\_Royal\_Microscopical\_Society* 170 (2), 229–236.
- Wan, Y., McDole, K., Keller, P.J., 2019. Light-sheet microscopy and its potential for understanding developmental processes. *Annu. Rev. Cell Dev. Biol.* 35, 655–681. <https://doi.org/10.1146/annurev-cellbio-100818-125311>.
- Wang, F., Wan, H., Ma, Z., Zhong, Y., Sun, Q., Tian, Y., Qu, L., Du, H., Zhang, M., Li, L., Ma, H., Luo, J., Liang, Y., Li, W.J., Hong, G., Liu, L., Dai, H., 2019. Light-sheet microscopy in the near-infrared II window. *Nat. Methods* 16, 545–552. <https://doi.org/10.1038/s41592-019-0398-7>.
- Weber, M., Huisken, J., 2011. Light sheet microscopy for real-time developmental biology. *Curr. Opin. Genet. Dev.* 21, 566–572. <https://doi.org/10.1016/j.jgde.2011.09.009>.
- Wolf, S., Supatto, W., Debrégeas, G., Mahou, P., Kruglik, S.G., Sintes, J.M., Beaupaire, E., Candelier, R., 2015. Whole-brain functional imaging with two-photon light-sheet microscopy. *Nat. Methods* 12, 379–380. <https://doi.org/10.1038/nmeth.3371>.
- Wu, Y., Chandris, P., Winter, P.W., Kim, E.Y., Jaumouillé, V., Kumar, A., Guo, M., Leung, J.M., Smith, C., Rey-Suarez, I., Liu, H., Waterman, C.M., Ramamurthi, K.S., La Riviere, P.J., Shroff, H., 2016. Simultaneous multiview capture and fusion improves spatial resolution in wide-field and light-sheet microscopy. *Optica* 3, 897. <https://doi.org/10.1364/optica.3.000897>.
- Wu, Y., Ghitani, A., Christensen, R., Santella, A., Du, Z., Rondeau, G., Bao, Z., Colón-Ramos, D., Shroff, H., 2011. Inverted selective plane illumination microscopy (iSPIM) enables coupled cell identity lineaging and neurodevelopmental imaging in *Caenorhabditis elegans*. *Proc. Natl. Acad. Sci. U.S.A.* 108, 17708–17713. <https://doi.org/10.1073/pnas.1108494108>.
- Wu, Y., Wawrzusin, P., Senseney, J., Fischer, R.S., Christensen, R., Santella, A., York, A.G., Winter, P.W., Waterman, C.M., Bao, Z., Colón-Ramos, D.A., McAuliffe, M., Shroff, H., 2013. Spatially isotropic four-dimensional imaging with dual-view plane illumination microscopy. *Nat. Biotechnol.* 31, 1032–1038. <https://doi.org/10.1038/nbt.2713>.
- Young, A.T., 1981. 8 Rayleigh scattering - a T young - appl opt 1981. *Appl. Opt.* 20, 533–535.